agriculture

MDPI

Article

Experimental and Numerical Analysis of Straw Motion under the Action of an Anti-Blocking Mechanism for a No-Till Maize Planter

Qingyi Zhang [1,2,3], Huimin Fang [1,2,3,*], Gaowei Xu [4], Mengmeng Niu [5] and Jinyu Li [1]

[1] School of Agricultural Engineering, Jiangsu University, Zhenjiang 212013, China; zhangqingyi@ujs.edu.cn (Q.Z.); 2212316040@stmail.ujs.edu.cn (J.L.)
[2] Key Laboratory for Theory and Technology of Intelligent Agricultural Machinery and Equipment, Jiangsu University, Zhenjiang 212013, China
[3] Jiangsu Province and Education Ministry Co-Sponsored Synergistic Innovation Center of Modern Agricultural Equipment, Zhenjiang 212013, China
[4] Department of Automotive Engineering, Shandong Jiaotong University, Jinan 250357, China; 202107@sdjtu.edu.cn
[5] Field Operation Technology and Equipment Innovation Center, Shandong Academy of Agricultural Machinery Sciences, Jinan 250100, China; moonniu@126.com
* Correspondence: fanghuimin@ujs.edu.cn; Tel.: +86-155-0860-2886

Abstract: To address the low clearance rate issue of the anti-blocking mechanism for maize no-till planters in the Huang-Huai-Hai Plain of China, experiments and simulations were conducted to analyze the individual and collective movements of straw under the action of the round roller-claw anti-blocking mechanism. A tracer-based measurement method for straw displacement was applied firstly. Experimental results showed that the straw forward displacement could be characterized by the average horizontal displacements of longitudinal and lateral tracers, while the straw side displacement could be characterized by the lateral displacement of the longitudinal tracer. The straw forward displacement was 58.95% greater than the side displacement. Forward, side, and total displacements of straw increased as the mechanism's forward speed increased from 3 km/h to 7 km/h, with corresponding rates of increase at 233.98%, 43.20%, and 162.47%, respectively. Furthermore, a model of straw–soil–mechanism interaction was constructed in EDEM 2022 software. The relative error between experimental and simulated straw clearance rates was 11.20%, confirming the applicability of the simulation model for studying straw–soil–mechanism interaction. Based on the simulation model, three straw tracers of different lengths were selected to study the motion behavior of straw. It was inferred that despite differences in straw length, the movement behaviors of the three straw tracers under the influence of the anti-blocking mechanism were similar. Additionally, longer straws exhibited greater displacements in all directions. This paper serves as a reference for studying straw motion behavior influenced by anti-blocking mechanisms.

Keywords: no-till planting; anti-blocking mechanism; straw displacement; tracer technology; discrete element method; straw clearance rate; straw motion behavior

Citation: Zhang, Q.; Fang, H.; Xu, G.; Niu, M.; Li, J. Experimental and Numerical Analysis of Straw Motion under the Action of an Anti-Blocking Mechanism for a No-Till Maize Planter. *Agriculture* **2024**, *14*, 1001. https://doi.org/10.3390/agriculture14071001

Academic Editors: Xiaojun Gao, Qinghui Lai and Tao Cui

Received: 15 May 2024
Revised: 19 June 2024
Accepted: 23 June 2024
Published: 26 June 2024

1. Introduction

The Huang-Huai-Hai Plain in China is characterized by semi-arid and semi-humid climates, with the predominant agricultural practice being the rotation of winter wheat and summer maize crops. With the continuous improvement in crop yields in recent years, there has been a corresponding increase in the production of straw [1]. However, an increasing amount of straw is being either discarded or openly burned, leading to significant resource wastage and a range of associated issues such as atmospheric pollution and traffic disruptions [2].

Incorporating crop residue cover, as a fundamental tenet of conservation agriculture, offers multifaceted benefits. It not only enhances straw utilization efficiency and mitigates pollution [3] but also mitigates soil erosion [4], enhances the physico-chemical properties of soil [5], and boosts crop yield [6]. However, the presence of straw residue covers poses challenges to maize planting in the Huang-Huai-Hai Plain. Maize planters are prone to blockages, leading to poor planting possibility and sowing quality [7]. Anti-blocking maize planters play a crucial role in ensuring efficient seeding and high sowing quality [8]. An effective anti-blocking mechanism is essential for mitigating straw blockages and enhancing the sowing reliability of maize planters.

Various types of anti-blocking mechanisms are designed to perform tasks such as chopping residues ahead and along the planting path, pushing residues sideways, or burying residues in a strip ahead of furrow opening. Recent developments in anti-blocking mechanisms include an oblique anti-blocking device [9], a round roller-claw anti-blocking mechanism [10], a spiral discharge anti-blocking and row-sorting device [11], a bionic shifting and diffluence straw anti-blocking device [12], and a combined stubble burying and anti-blocking device [13]. These anti-blocking mechanisms find applications in rapeseed direct planting as well as corn no-tillage planting. Theoretical [14,15], experimental [16,17], and numerical [18,19] methods are employed to assess the performance of anti-blocking mechanisms in terms of soil disturbance and straw cleaning rate. For instance, Li et al. [14] analyzed the performance of symmetrical spiral row-sorting of the straw device with a theoretical method, Jiang et al. [16] tested the performance of a seedbed preparation machine before transplanting of rapeseed with a combined transplanter in the field, and Zhu et al. [18] optimized the structural parameters of the bionic shifting and diffluence straw anti-blocking mechanism via EDEM 2022 software. However, these studies focused on the design and optimization of the anti-blocking mechanism. There is a lack of attention to the interaction between straw and the anti-blocking mechanism.

The interaction between straw and agricultural implements is crucial for developing effective anti-blocking mechanisms, and the interaction is usually characterized by straw movement [20]. Researchers employ various methods to analyze straw movement, including theoretical analysis, advanced testing, numerical simulations, and experiments. Gu et al. [21] demonstrated the effectiveness of the "laminar flow splitter" due to its property of round-flow. Gao et al. [22] designed an anti-blocking mechanism, combining a driven divider with a passive residue separating device based on the theory of the boundary layer in fluid mechanics. Liao et al. [23] tracked the movement and throwing trajectory of straws, cut down by the saw-tooth anti-blocking mechanism of a no-tillage planter, with the help of high-speed photography. Niu et al. [15] studied individual and group straw movement numerically. Fang et al. [20] evaluated anti-blocking devices through experiments and simulations. Some studies utilized high-speed cameras [9] and tracer technology [10] to observe straw movement but lacked detailed explanations. Understanding straw motion requires clarity on how anti-blocking devices control and guide it, an aspect currently under-researched in straw–soil–mechanism interaction studies.

In order to address the dilemma of our unclear understanding of straw motion under the influence of anti-blocking mechanisms, a controlled soil bin experiment and discrete element simulation were conducted to achieve the following objectives: (i) propose a measurement method for straw displacement and investigate the effects of working parameters of the anti-blocking mechanism on straw displacement via an experiment; (ii) validate the simulation model of straw–soil–mechanism interaction, and analyze the motion behavior of straw based on simulation.

2. Materials and Methods

2.1. Description of Anti-Blocking Mechanism

The anti-blocking furrow opener, depicted in Figure 1a, is constructed from steel and affixed to a maize planter, specifically tailored for no-tillage sowing in the Huang-Huai-Hai Plain. A pivotal component of this furrow opener is the round roller-claw anti-

blocking mechanism, illustrated in Figure 1b. This mechanism has the capability to rotate horizontally under power while advancing alongside the anti-blocking furrow opener. The geometrical characteristics of the anti-blocking mechanism, as outlined in Table 1, were employed for its shape and design.

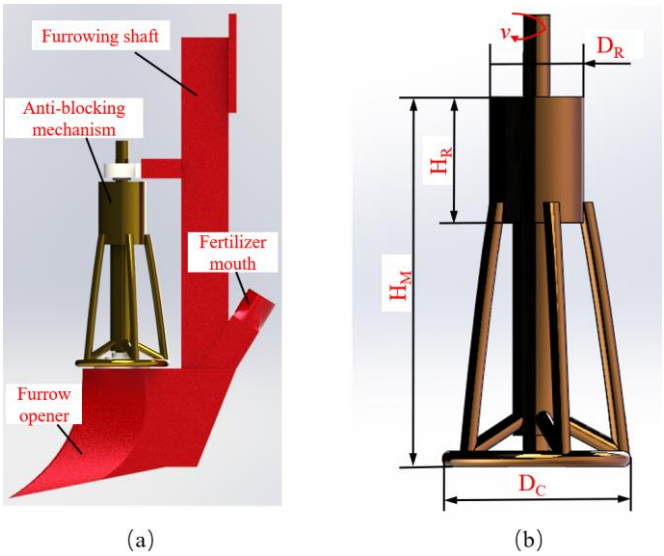

Figure 1. Experimental mechanism: (**a**) furrow opener; (**b**) anti-blocking mechanism.

Table 1. Characteristics of a round roller-claw anti-blocking mechanism.

Parameters	Values
Height of whole mechanism H_M/(mm)	234
Height of round roller H_R/(mm)	80
Biggest diameter of claw D_C/(mm)	120
Diameter of round roller D_R/(mm)	60

2.2. Experimental Design

2.2.1. Description of Soil Bin Experiment

The indoor experiments, depicted in Figure 2, were carried out in the soil bin at the Shandong Academy of Agricultural Machinery Sciences, located in Shandong Province, People's Republic of China (China). The dimensions of soil bin are 60 m × 2.5 m × 1 m (length × width × depth) and it is filled with sufficient soil, enabling the testing of the maize planter. The maize planter was propelled by a PTO shaft of the soil bin tester, while two sets of gear reducers facilitated the rotational motion of the anti-blocking mechanism. The soil density was managed at 1.70 g/cm^3 with the average moisture content of the 0–5 cm soil layer as 10.07%, and 13.51% for the next 5 cm soil depth. The soil hardness was 0.96 MPa.

The straw was uniformly distributed across the soil surface, creating a coverage area of straw measuring 1 m in width and 20 m in length, ensuring that the anti-blocking mechanism moved forward in the middle of the straw row. The wheat straw used in the experiments was harvested from fields in Shandong Province, China, with an average mulching quantity of 610 kg/mu.

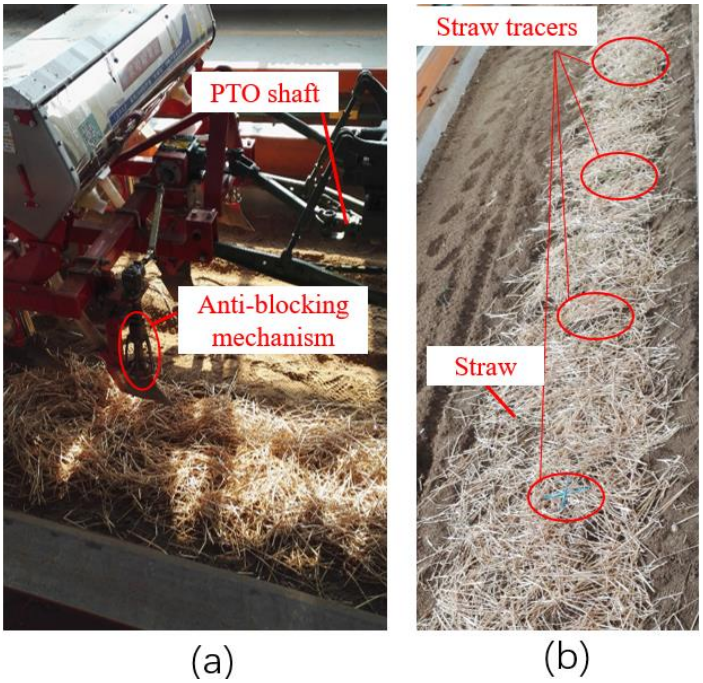

Figure 2. Experimental site in soil bin: (**a**) experimental equipment; (**b**) straw distribution.

2.2.2. Description of Straw Tracer

Five groups of straw tracers were positioned in the test sample area, which were painted purple, blue, red, green, and black, respectively. Each group of straw tracers was spaced 1 m apart to avoid motion interference. Two straw tracers with same color were utilized, with one aligned parallel to the forward motion of the anti-blocking mechanism, termed the longitudinal straw tracer. The other straw tracer, placed perpendicular to it, was called the lateral straw tracer. Every set of longitudinal and lateral straw tracers shared the same color, where the lateral straw tracers were distinguished by special markings at both ends. Three sets of straw tracers (purple, red, and black) were positioned along the forward trajectory of the anti-blocking mechanism, while the remaining two sets (blue and green) were placed laterally, offset by 30 mm from the forward path. The arrangement of the straw tracers is illustrated in Figure 3.

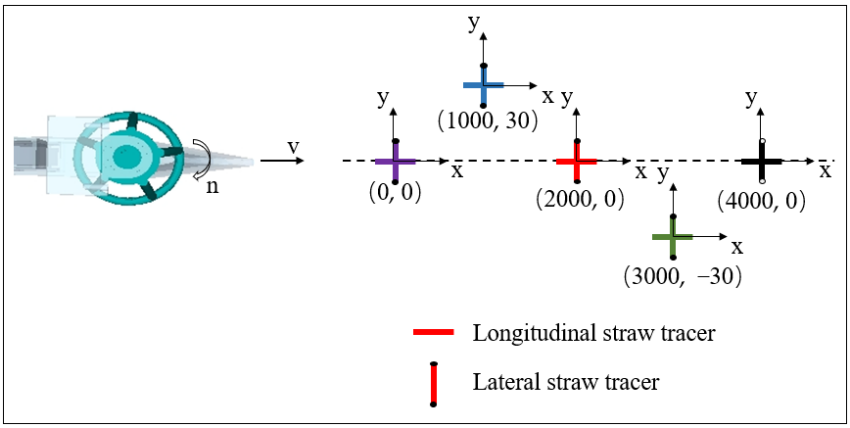

Figure 3. Schematic view of straw tracer placements. Note: v represents the forward velocity, km/h; n represents the rotational speed of the anti-blocking mechanism, r/min.

2.2.3. Measurement

(A) Straw displacement

Straw displacement refers to the movement of straw in both horizontal and lateral directions. It is determined by calculating the absolute difference between the initial and final positions of straw tracers.

(B) Straw clearance rate

The straw clearance rate quantifies the change in the quantity of straw within a 60 mm range on either side of the anti-blocking mechanism forward path. It is calculated as the ratio of the difference in straw weight before and after the anti-blocking mechanism's operation to the initial straw weight within this specified range.

2.3. Simulation Design

2.3.1. Description of Simulation Model

The simulation model of straw–soil-mechanism interaction was developed using EDEM 2022 (Version 8.0.0, Altair Engineering, Inc., Troy, MI, United States). Hard spheres of 5 mm radius were used to represent soil particles, and the contact model between soil particles was based on the Hertz–Mindlin bonding model. Hard spheres with a radius of 3 mm were used to represent straw particles, with a space of 5 mm separating adjacent straw particles.

Considering the actual length of the straw in the field and the size of the straw particles, three lengths of 36, 76, and 116 mm, respectively, were used to model the straw in this study. The 7, 15, and 23 spheres, respectively, were connected to form the 36, 76, and 116 mm straw, respectively. There were 60,000 soil particles and 2400 straw particles, with three lengths of 36 mm, 76 mm, and 116 mm, respectively, generated randomly. According to the previous work [10], the material properties and interaction parameters used in this simulation were as detailed in Table 2. Figure 4 illustrates this simulation model.

Table 2. Simulation parameters.

Parameters	Values
Density of soil/(gm^{-3})	1.85
Density of straw/(gm^{-3})	0.24
Density of steel/(gm^{-3})	7.87
Poisson ratio of soil	0.38
Poisson ratio of straw	0.4
Poisson ratio of steel	0.3
Shear modules of soil/(Pa)	1×10^6
Shear modules of straw/(Pa)	1×10^6
Shear modules of steel/(Pa)	7.9×10^{10}
Recovery coefficient of soil–soil	0.6
Recovery coefficient of soil–steel	0.6
Recovery coefficient of straw–steel	0.3
Static fiction coefficient of soil–soil	0.6
Static fiction coefficient of soil–steel	0.6
Static fiction coefficient of straw–steel	0.3
Rolling fiction coefficient of soil–soil	0.4
Rolling fiction coefficient of soil–steel	0.05
Rolling fiction coefficient of straw–steel	0.01

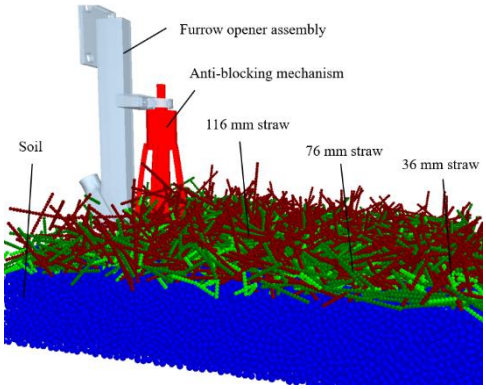

Figure 4. Simulation model of straw–soil-mechanism interaction.

2.3.2. Description of Straw Tracer

In the simulation, 2400 straw particles were randomly generated on the soil surface. Straws of different lengths were chosen as the straw tracer to assess and analyze the displacement of a single piece of straw by monitoring its movement. As straw was randomly distributed on the soil surface, it was essential to compare the differences in the motion behavior of straw at the same location. There are two principles for selecting the three straw tracers. Firstly, tracers should align closely with the forward path of the anti-blocking mechanism, maintaining consistency in the X coordinate values. Secondly, maintaining consistent relative heights of the tracers ensures uniformity in the Y coordinate values, that is, the Y coordinate values are as consistent as possible. Based on these principles, the selected straw tracers and their relative positions in the anti-blocking mechanism are as shown in Figure 5.

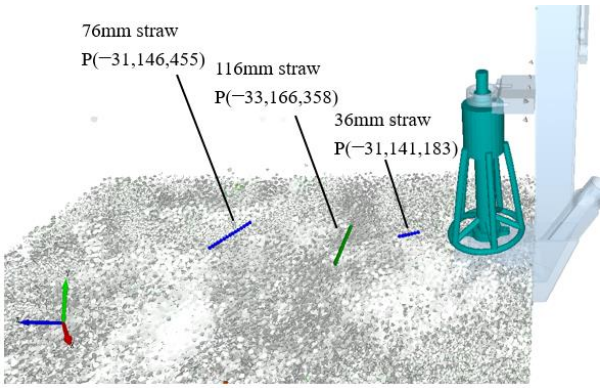

Figure 5. The straw tracers in the simulation and their positions.

2.3.3. Measurement

(A) Straw movement

The positions of three straw tracers were continuously monitored at every instance, utilizing the established model for full coverage of straw distribution. Straw movement refers to the positional changes in straw in both horizontal and lateral directions. The simulation characterizes straw movement by observing the fluctuations in tracer positions over time.

(B) Straw clearance rate

We chose a 60 mm span on either side of the anti-blocking mechanism as the designated area for analyzing straw clearance in the simulation. The straw clearance rate is defined as the ratio of the difference in the straw quantity before and after simulation to the initial straw quantity.

2.4. Experimental and Numerical Treatment Design

Three sets of experiments and simulation were designed and conducted in this study. In the first group of experiments, the orientation and position of the straw tracers were evaluated to determine their impact on straw displacement based on the soil bin test. Additionally, the method for measuring straw displacement was established. Subsequently, the effect of the operational parameters of the anti-blocking mechanism (forward and rotational speed) on straw displacement (forward, side, and total displacement) was investigated using the established measurement technique. This experimental set included three sets of forward speeds (3, 5, and 7 km/h) and four sets of rotational speeds (260, 400, 530, and 740 r/min).

The second experiment focused on using the straw clearance rate to characterize straw side movement. The verification of the simulation model was assessed by comparing the difference in the straw clearance rate between simulation and experimental results. This experiment involved five sets of forward speeds (3, 5, 7, 8, and 9 km/h) while maintaining a constant rotational speed of 400 r/min.

In the simulation, three different straw lengths (36 mm, 76 mm, and 116 mm) positioned approximately at the same location were chosen for motion tracking based on the simulation model. This numerical treatment aimed to analyze the motion behavior of straw under constant conditions of rotational speed (400 r/min) and forward speed (7 km/h).

2.5. Statistical Analysis

Detection of significant differences among the results was performed through analysis of variance using SPSS ver.23 [24]. A significance level of 0.05 in a Duncan test was adopted in this study [25].

3. Results and Discussions

3.1. Measurement Method of Straw Displacement

3.1.1. Effect of Tracer Orientations on Straw Displacement

Longitudinal and lateral orientations were observed for all straw tracers during the experiment. Forward and side straw displacements, measured using longitudinal and lateral tracers, are depicted in Figure 6. The round roller-claw anti-blocking mechanism was tested at rotational speeds of 260, 400, 530, and 740 r/min, respectively, along with three forward speeds of 3, 5, and 7 km/h.

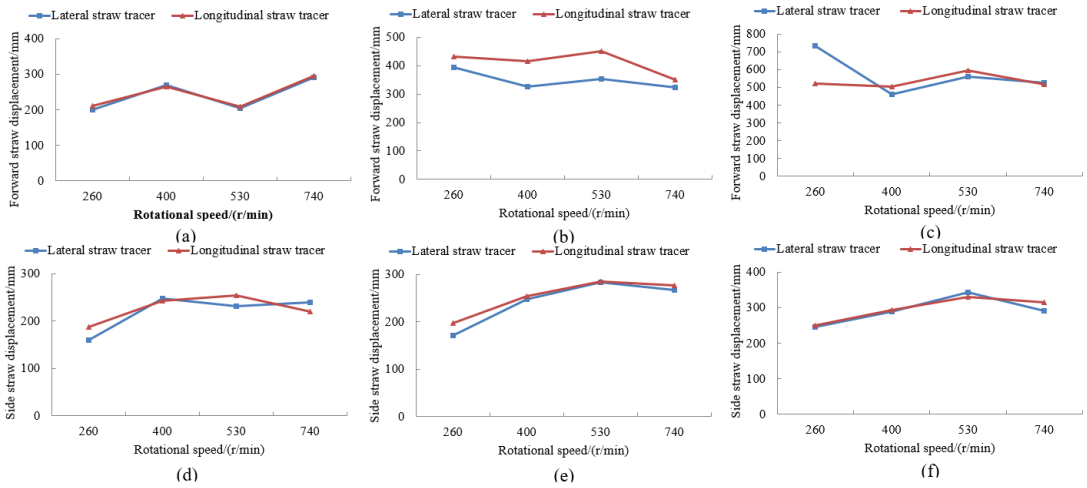

Figure 6. Straw displacements measured with longitudinal and lateral straw tracers: (**a**,**d**) straw forward and side displacements under forward speeds of 3 km/h; (**b**,**e**) straw forward and side displacements under forward speeds of 5 km/h; (**c**,**f**) straw forward and side displacements under forward speeds of 7 km/h.

Figure 6a–c depicts the forward displacement of straw measured by tracers placed both longitudinally and laterally under varying operational conditions. The discrepancy between the measurements was minimal at a forward speed of 3 km/h (Figure 6a), exhibiting an average absolute difference of 6.2 mm and an average relative difference of 2.8%. However, at a forward speed of 5 km/h (Figure 6b), the disparity peaked, with an average absolute difference of 63.1 mm and an average relative difference of 18.3%. Notably, at a forward speed of 7 km/h, a notable difference emerged only when the anti-blocking mechanism operated at a rotational speed of 260 rpm, resulting in an absolute difference of 212 mm, possibly attributable to considerable error induced by straw dragging [26]. Additionally, the average absolute error under varying operating parameters was 29.22 mm, with a relative error of 5.83%. The side displacement of straw, as depicted in Figure 6d–f, was measured using tracers positioned both longitudinally and laterally across various operational settings. The comparison revealed a slight disparity between the measurements obtained from the two placement strategies, showing an average absolute difference of 13.93 mm and a relative difference of 5.83%.

The analysis suggested that tracers employing the two placement strategies manifest noteworthy errors in assessing forward displacement, which ought to be the mean of both. Nonetheless, the discrepancy in side displacement measurement was insignificant. Hence, longitudinal straw tracers are recommended for side displacement measurement, aligning with the findings of Fang et al. [26], that is, when studying the straw displacement under the action of a rotating component, the straw forward displacement can be obtained by considering the average horizontal displacements of longitudinal and lateral tracers, and the straw side displacement can be obtained by considering the lateral displacement of the longitudinal tracer.

3.1.2. Effect of Tracer Positions on Straw Displacement

Using straw tracers positioned variably to measure both forward and side displacements of straw, the effects of the tracer position on straw displacements were ascertained, as depicted in Figure 7.

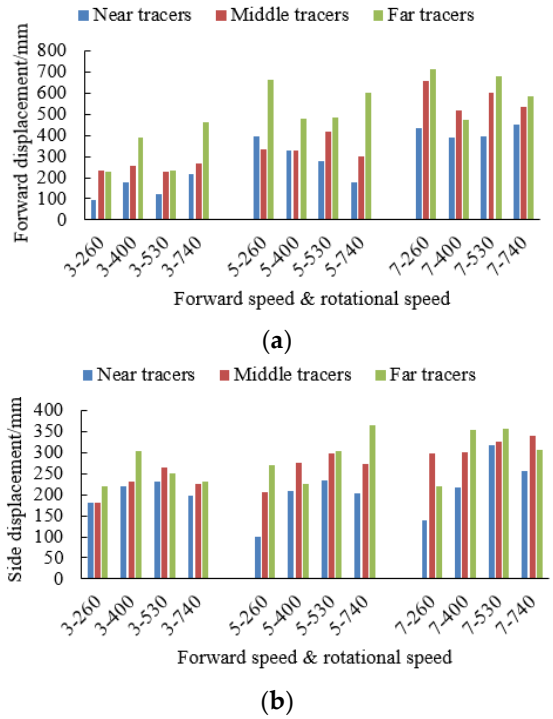

Figure 7. Straw displacements measured with straw tracers at different positions: (**a**) the forward straw displacement measured with straw tracers at different positions; (**b**) the side straw displacement measured with straw tracers at different positions.

The anti-blocking mechanism induces horizontal movement in straw as it advances. Additionally, the rotating mechanism throws straw tangentially, resulting in a combined motion in both horizontal and lateral directions. A comparison of straw displacements in the horizontal and lateral directions reveals that lower forward and rotational speeds of the anti-blocking mechanism result in smaller side displacements of the nearby straw tracer. Furthermore, the side displacement of straw was generally less than the forward displacement, aligning with previous research findings [27]. This phenomenon primarily occurs due to the straw's low side component velocity upon being thrown tangentially by the mechanism, coupled with constraints from surrounding straw.

Straw tracers placed at various positions experience distinct forces from the anti-blocking mechanism and surrounding straw, leading to variations in straw displacement. Both forward and side displacements followed a consistent trend, where the straw tracer at the distant position showed the highest displacement, followed by the middle position, and finally, the nearby position had the smallest displacement. This is attributed to the motion of straw under the influence of the anti-blocking mechanism resembling fluid flow; hence, straw at distant positions experiences larger displacements as it is situated at the periphery of the fluid. Using the displacement measured by the middle-position straw tracer as the control, the average forward displacement of the distant-position straw tracer exceeded that of the middle position by 28.37%, while the middle-position tracer's displacement was 25.75% higher than the nearby tracer. In the lateral direction, the side displacement measured by the straw tracer at the distant position was 5.95% higher than that measured by the straw tracer at the middle position, and the side displacement of the middle-position tracer was 22.07% higher than that of the nearby tracer. Concerning various forward speeds of the anti-blocking mechanism, the forward displacements measured by the distant-position straw tracer were 34.03%, 61.94%, and 5.98% higher than those of the middle position, while the middle-position tracer's displacements were 37.66%, 14.18%, and 27.59% higher than those of the nearby tracer at forward speeds of 3, 5, and 7 km/h. In terms of side displacement, the straw tracer in the middle position showed displacements 8.26%, 28.89%, and 26.26% higher than those of the nearby tracer, respectively, at forward speeds of 3, 5, and 7 km/h. Side displacements measured by the distant-position straw tracer were 11.34% and 10.79% higher than those measured by the middle-position straw tracer at forward speeds of 3 and 5 km/h, respectively. At a forward speed of 7 km/h, the distant position straw tracer's displacements were marginally (1.94%) less than those of the middle-position straw tracer.

Furthermore, upon comparing the average displacements of the straw tracers at distant and nearby positions with the displacement obtained by the straw tracer in the middle position, it was found that the relative errors in forward and side displacements under various operating parameters of the anti-blocking mechanism were 21.25% and 12.35%, respectively. At a forward speed of 3 km/h for the anti-blocking mechanism, the difference in forward displacement between them exhibited no discernible pattern with variations in the rotational speed of the anti-blocking mechanism. This observation was consistent for side displacement as well, with relative errors in forward and side displacements at 23.06% and 9.75%, respectively. When the forward speed of the anti-blocking mechanism was 5 km/h, the mean forward displacement of the straw tracers at distant and nearby positions was 29.95% higher than that of the straw tracer in the middle position, while the mean side displacement was 11.14% lower than that of the straw tracer in the middle position. At a forward speed of 7 km/h for the anti-blocking mechanism, the average forward displacement of the straw tracers at distant and nearby positions was 10.73% less than that of the straw tracer in the middle position. Moreover, the side displacement of the two exhibited no apparent correlation with alterations in the rotational speed of the anti-blocking mechanism, with a relative error of 16.16%.

Hence, to comprehensively account for the impact of straw tracers at distinct positions on straw displacement and to better reflect the actual dynamics of straw movement, this research adopted the mean displacements of straw tracers at varied positions as repre-

sentative values for straw displacement. The straw tracers were generally not placed in different positions in previous studies [26,27], and this study provides a straw displacement measurement method to reduce measurement errors caused by the position of straw tracers. Specifically, the mean forward displacement of straw tracers at distant, middle, and nearby positions will serve as the horizontal displacement metric for straw, while the mean side displacement of straw tracers in the same positions will function as the corresponding side displacement metric.

3.2. Straw Displacement Influenced by the Working Parameters of the Mechanism

Following the harvest of the wheat crop, the straw is distributed across the field, after which maize seeding is conducted directly. If the straw cannot be pushed ahead and sideways, the maize planter is prone to blockages. Assessing the impact of operational parameters on straw displacement is crucial for evaluating the effectiveness of the anti-blocking mechanism [10]. Figure 8 displays the forward, side, and total straw displacement under various rotational speeds (260, 400, 530, and 740 rpm) and forward speeds (3, 5, and 7 km/h) of the anti-blocking mechanism. Apart from instances where the straw forward displacement was marginally less than the side displacement at a forward speed of 3 km/h and a rotational speed of 530 rpm, the forward displacement consistently exceeded the side displacement across all operational parameters of the anti-blocking mechanism. The average absolute value of displacement was 155 mm, with a relative difference of 58.95%.

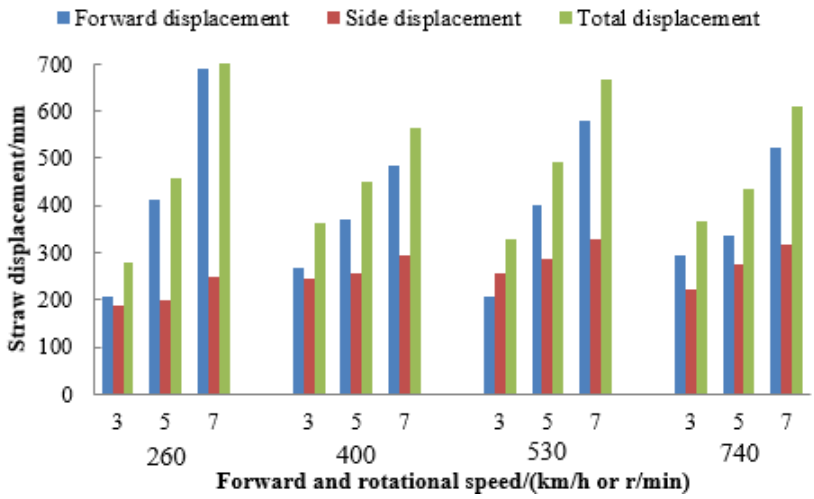

Figure 8. The forward straw displacement measured in different forward and rotational speed conditions.

Forward displacement of straw increased with the forward speed of the mechanism, which maintained consistency across all four rotational speeds of the anti-blocking mechanism. a lower rotational speed of the anti-blocking mechanism correlated with a higher increase in the straw forward displacement rate. At a rotational speed of 260 rpm, the forward displacement increased by 100.49% when the forward speed changed from 3 km/h to 5 km/h, and by 233.98% when the forward speed increased from 3 km/h to 7 km/h. Nevertheless, no consistent pattern emerged in the straw forward displacement variations with rotational speed at a constant forward speed of the mechanism.

Regarding side displacement, straw displacement increased with forward speed, consistent across all four rotational speeds of the anti-blocking mechanism. A higher rotational speed of the anti-blocking mechanism correlated with a greater increase in straw side displacement rate. At a rotational speed of 740 rpm, side displacement increased by 25.38% as the forward speed changed from 3 km/h to 5 km/h, and by 43.20% as the forward speed increased from 3 km/h to 7 km/h. Nevertheless, no consistent pattern emerged in straw side displacement variations with rotational speed at a constant forward speed of the mechanism.

Concerning total displacement, straw displacement rose with an increasing forward speed of the mechanism at constant rotational speeds of the anti-blocking mechanism, consistent across all four rotational speeds. Since forward displacement of straw consistently exceeded side displacement, the trend in total straw displacement mirrored that of forward displacement. Thus, a lower rotational speed of the anti-blocking mechanism resulted in a higher rate of increase in total straw displacement. At a rotational speed of 260 rpm, total displacement increased by 64.23% as the forward speed changed from 3 km/h to 5 km/h, and forward displacement increased by 162.47% as the forward speed increased from 3 km/h to 7 km/h. Nevertheless, there was no discernible pattern in the variations in total straw displacement with rotational speed at a constant forward speed of the mechanism.

3.3. Verification of the Numerical Model and Straw Motion Analysis

3.3.1. Verification of the Simulation Model Based on the Straw Clearance Rate

The straw clearance rate might be more suitable to describe straw side movement because it represents the movement behavior of a group of pieces of straw in a defined specific area, while the straw side displacement was measured only by specific straw tracers. The experimental and simulation results of straw clearance rates with different forward speeds are shown in Figure 9, where the rotational speed of the anti-blocking mechanism is 740 rpm.

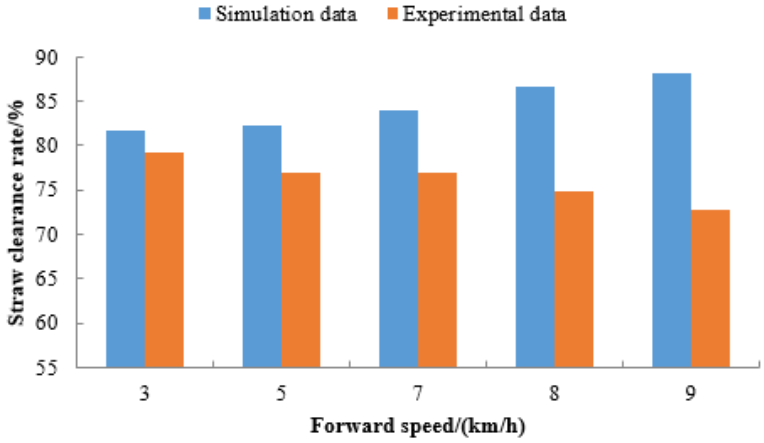

Figure 9. Comparison of straw clearance rates between simulation and experimental results.

The straw clearance rate decreased with the increase in the forward speed of the anti-blocking mechanism in the experiment. The forward speed was too fast for the straw to be ejected from the furrow in time when it moved outward with the anti-blocking mechanism. This also indicated that the straw would remain in the furrow when the ratio of circumferential velocity to forward velocity was large. However, the decrease in the proportion of straw clearance rate with the increase in the forward speed of the mechanism was not significant; the straw clearance rate only increased by 8.17% when the forward speed increased from 3 km/h to 9 km/h.

In the simulation, the straw clearance rate increased with the increase in the forward speed of the anti-blocking mechanism. Additionally, the straw clearance rate only increased by a small margin (7.84%) when the forward speed increased from 3 km/h to 9 km/h. There was a different trend in straw clearance rate variation between the simulation and experimental results, which might be because the straw in the simulation was rigid and did not intertwine and clump together while moving with the anti-blocking mechanism. But during the experiment, where the straw could become entangled and compressed when the forward speed was high, this phenomenon made the straw difficult to eject. The difference in straw clearance rates the between simulation and experimental results might indicate that rigid straw was ejected more easily.

Although the simulation straw clearance rates under various operating parameters were higher than the experimental data, the discrepancies were relatively minor. The average relative error between the experimental and simulation straw clearance rates was 11.20%, with the minimum error (2.99%) occurring at a forward speed of 3 km/h for the anti-blocking mechanism, and the maximum error (20.95%) occurring at a forward speed of 9 km/h. The relative error increased with the increase in the forward speed of the mechanism, indicating that the assumption of rigid straw in the simulation had a greater impact when the forward speed of the mechanism was high. However, the small differences in their values also indicated that the simulation model was suitable for studying the interaction between straw and the anti-blocking mechanism, especially at a lower forward speed (less than 7 km/h, where the error is 9.11%). Therefore, subsequent simulations of straw motion were based on a forward speed of 7 km/h for the anti-blocking mechanism.

3.3.2. Analysis of Individual Straw Movement Behaviors

Three straw tracers, each of different lengths, were selected to track their motion during the simulation. At the beginning of the simulation, all three straws were stationary and were located on the ground in front of the anti-blocking mechanism. Subsequently, under the combined effect of the anti-blocking mechanism and the surrounding straw, they ascended along the rotation direction of the mechanism at a certain speed. Afterwards, the straws were ejected under the increasing centrifugal force and decreasing support force of the straw bed. The changes in the position of the straw in the side, forward, and vertical directions are shown in Figure 10. From the figure, it is evident that although the lengths of the straws are different, their motion behaviors under the action of the anti-blocking mechanism are similar.

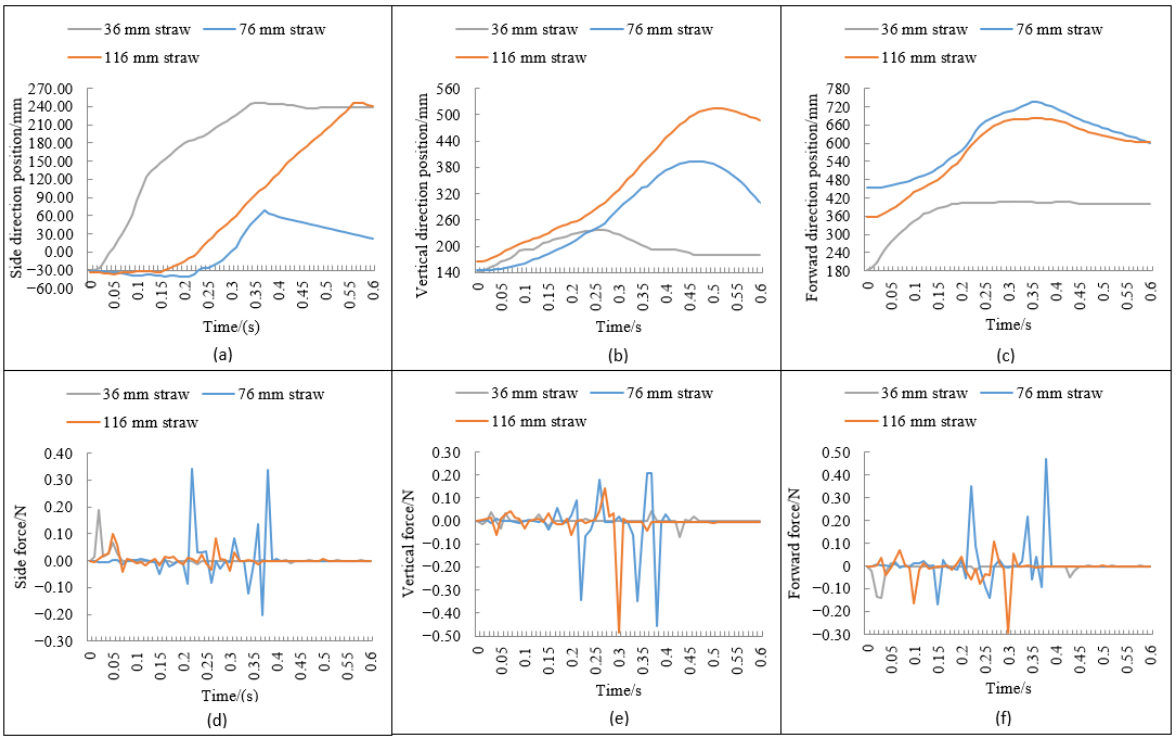

Figure 10. The movement and force of selected straws: (**a**–**c**) the movement trajectory of straw in the side, vertical, and forward directions over time; (**d**–**f**) the force exerted on straw in the side, vertical, and forward directions over time.

In the side direction, the straws moved along the rotation direction of the anti-blocking mechanism and were subsequently ejected. This phenomenon was similar to the motion behavior of straw under the action of rotating mechanisms [27]. The side displacements of the longer and shorter straws were similar, while that of the medium-length straw was the smallest. The shortest straw (36 mm) rapidly moved approximately 280 mm laterally under the influence of the anti-blocking mechanism and then remained nearly stationary thereafter. The longest straw (116 mm) did not exhibit as drastic a movement as the shortest straw (36 mm) but had approximately equal side displacements. The smallest side displacement of the medium-length straw might be due to the inhibiting effect of the surrounding dense straw.

In the vertical direction, the straws exhibited climbing behavior under the influence of the anti-blocking mechanism. This proved that the mechanism with a small-diameter upper and large-diameter lower structure would lift the straw during rotation [15]. Moreover, the climbing behavior was more pronounced and the climbing duration longer for the longer straw. The shortest straw only climbed approximately 95 mm before descending, while the medium-length and the longest straw climbed 248 mm and 348 mm, respectively. The vertical motion of the straw tracers confirmed the functionality of the anti-blocking mechanism in guiding the straw to climb.

In the horizontal direction, the straw moved forward under the influence of the anti-blocking mechanism. All straws of different lengths moved forward under the push of the mechanism initially. Subsequently, the medium-length straw and the longest straw exhibited backward behavior after losing the guiding effect of the mechanism. The continuous backward movement behavior indicated that the straw formed a smooth flow under the action of the mechanism. Additionally, the longer the straw, the greater the distance it travelled; for example, the 116 mm straw moved 325 mm in the forward direction.

4. Conclusions

A tracer-based measurement method was applied to investigate the impact of operational parameters of the anti-blocking mechanism on straw displacement. Then, a straw–soil-mechanism interaction model was developed using EDEM 2022 software. The model's feasibility was confirmed from the perspective of straw clearance rates. Furthermore, the model was used to study the individual motion behavior of straw over time under the influence of the anti-blocking mechanism. The research results showed that the tracer method could be used to study the straw displacement under the action of the anti-blocking mechanism. The experimental results also indicated that the forward displacement, side displacement, and total displacement of the straw increased with the increase in the forward speed of the mechanism at a constant speed of rotation. The straw–soil–mechanism interaction model could be used to study the motion behavior of straw. Straws in different positions had similar movement behaviors under the action of the anti-blocking mechanism. The motion behavior of straw under the anti-blocking mechanism offers insights into the interactions among straw, soil, and anti-blocking mechanisms.

Author Contributions: Conceptualization, Q.Z. and H.F.; methodology, Q.Z. and M.N.; software, Q.Z. and H.F.; validation, Q.Z., H.F. and G.X.; formal analysis, M.N. and J.L.; investigation, Q.Z., H.F., G.X. and M.N.; resources, H.F.; data curation, H.F.; writing—original draft preparation, Q.Z. and J.L.; writing—review and editing, H.F., G.X. and M.N.; visualization, Q.Z.; supervision, H.F.; project administration, H.F.; funding acquisition, H.F. All authors have read and agreed to the published version of the manuscript.

Funding: This research was funded by the China Postdoctoral Science Foundation, grant number 2023M741433, the Research Foundation for Talented Scholars of Jiangsu University, grant number 22JDG041, the Priority Academic Program Development of Jiangsu Higher Education Institutions, grant number PAPD-2023-87, and the Jiangsu University Agricultural Engineering Department Project, grant number NGXBTD20240307.

Institutional Review Board Statement: Not applicable.

Data Availability Statement: The analyzed datasets are available from the corresponding author on reasonable request.

Conflicts of Interest: The authors declare no conflicts of interest.

References

1. Li, W.; Zhang, C.; Ma, T.; Li, W. Estimation of summer maize biomass based on a crop growth model. *Emir. J. Food Agric.* **2021**, *33*, 742–750. [CrossRef]
2. Memon, M.S.; Chen, S.; Niu, Y.; Zhou, W.; Elsherbiny, O.; Liang, R.; Du, Z.; Guo, X. Evaluating the efficacy of sentinel-2B and landsat-8 for estimating and mapping wheat straw cover in rice-wheat fields. *Agronomy* **2023**, *13*, 2691. [CrossRef]
3. Guo, Y.; Cui, M.; Xu, Z. Spatial characteristics of transfer plots and conservation tillage technology adoption: Evidence from a survey of four provinces in China. *Agriculture* **2023**, *13*, 1601. [CrossRef]
4. Melland, A.R.; Antille, D.L.; Dang, Y.P. Effects of strategic tillage on short-term erosion, nutrient loss in runoff and greenhouse gas emissions. *Soil Res.* **2016**, *55*, 201–214. [CrossRef]
5. Tunio, M.H.; Gao, J.; Talpur, M.A.; Lakhiar, I.A.; Chandio, F.A.; Shaikh, S.A.; Solangi, K.A. Effects of different irrigation frequencies and incorporation of rice straw on yield and water productivity of wheat crop. *Int. J. Agric. Biol. Eng.* **2020**, *13*, 138–145. [CrossRef]
6. Khan, I.; Iqbal, B.; Khan, A.A.; Inamullah; Rehman, A.; Fayyaz, A.; Shakoor, A.; Farooq, T.H.; Wang, L. The interactive impact of straw mulch and biochar application positively enhanced the growth indexes of maize (*Zea mays* L.) crop. *Agronomy* **2022**, *12*, 2584. [CrossRef]
7. Ahmad, F.; Adeel, M.; Qiu, B.; Ma, J.; Shoaib, M.; Shakoor, A.; Chandio, F.A. Sowing uniformity of bed-type pneumatic maize planter at various seedbed preparation levels and machine travel speeds. *Int. J. Agric. Biol. Eng.* **2021**, *14*, 165–171. [CrossRef]
8. Zhang, X.; Li, H.; Du, R.; Ma, S.; He, J.; Wang, Q.; Chen, W.; Zheng, Z.; Zhang, Z. Effects of key design parameters of tine furrow opener on soil seedbed properties. *Int. J. Agric. Biol. Eng.* **2016**, *9*, 67–80.
9. Yao, W.; Diao, P.; Miao, H.; Li, S. Design and experiment of anti-blocking components for shallow stubble clearing based on soil bin test. *Agriculture* **2022**, *12*, 1728. [CrossRef]
10. Fang, H.; Niu, M.; Zhu, Z.; Zhang, Q. Experimental and numerical investigations of the impacts of separating board and anti-blocking mechanism on maize seeding. *J. Agric. Eng.* **2022**, *LIII*, 1273.
11. Li, Y.; Lu, C.; Li, H.; He, J.; Wang, Q.; Huang, S.; Gao, Z.; Yuan, P.; Wei, X.; Zhan, H. Design and experiment of spiral discharge anti-blocking and row-sorting device of wheat no-till planter. *Agriculture* **2022**, *12*, 468. [CrossRef]
12. Zhu, H.; Zhang, X.; Hong, Y.; Bai, L.; Zhao, H.; Ma, S. Design and experiment of bionic shifting and diffluence straw anti-blocking device. *Agric. Res. Arid Areas* **2023**, *41*, 318–328.
13. Du, W.; Zhou, G.; Zhang, Q.; Bian, Q.; Liao, Q.; Liao, Y. Design and experiment of the anti-blocking device combined stubble burying for rapeseed direct seeding. *Trans. Chin. Soc. Agric. Eng.* **2024**, *40*, 60–70.
14. Li, Y.; Lu, C.; Li, H.; Wang, Z.; Gao, Z.; Wei, X.; He, D. Design and experiment of symmetrical spiral row-sorting of the straw device based on kinematics analysis. *Agriculture* **2022**, *12*, 896. [CrossRef]
15. Niu, M.; Fang, H.; Chandio, F.A.; Shi, S.; Xue, Y.; Liu, H. Design and experiment of separating guiding anti-blocking mechanism for no-tillage maize planter. *Trans. Chin. Soc. Agric. Mach.* **2019**, *50*, 52–58.
16. Jiang, L.; Tang, Q.; Wu, J.; Yu, W.; Zhang, M.; Jiang, D.; Wei, D. Design and test of seedbed preparation machine before transplanting of rapeseed combined transplanter. *Agriculture* **2022**, *12*, 1427. [CrossRef]
17. Yao, W.; Zhao, D.; Miao, H.; Cui, P.; Wei, M.; Diao, P. Design and experiment of oblique anti-blocking device for no-tillage planter with shallow plowing stubble clearing. *Trans. Chin. Soc. Agric. Mach.* **2022**, *53*, 42–52.
18. Zhu, H.; Wu, X.; Qian, C.; Bai, L.; Ma, S.; Zhao, H.; Zhang, X.; Li, H. Design and experimental study of a bi-directional rotating stubble-cutting no-tillage planter. *Agriculture* **2022**, *12*, 1637. [CrossRef]
19. Wang, L.; Bian, O.; Liao, Q.; Wang, B.; Liao, Y.; Zhang, O. Burying stubble and anti-blocking deep fertilization composite device for rapeseed direct planting in high stubble and heavy soil rice stubble field. *Trans. Chin. Soc. Agric. Mach.* **2023**, *54*, 83–94.
20. Fang, H.; Shi, S.; Qiao, L.; Niu, M.; Xu, G.; Jian, S. Numerical and experimental study of working performance of round roller claw type anti-blocking mechanism. *J. Chin. Agric. Mech.* **2018**, *39*, 1–9.
21. Gu, Y.; Zhang, Y.; Song, J. A study on "laminar flow splitter" as blocking proofing device for mulching no-tillage planters. *Trans. Chin. Soc. Agric. Mach.* **1994**, *25*, 46–51.
22. Gao, N.; Zhang, D.; Yang, L.; Cui, T. Design of anti-blocking mechanism combined driven divider with passive residue separating device. *Trans. Chin. Soc. Agric. Mach.* **2014**, *45*, 85–91.
23. Liao, Q. Analysis on the saw-tooth anti-blocking mechanism for no-tillage planter by the high-speed photograph technology. *Trans. Chin. Soc. Agric. Mach.* **2005**, *26*, 46–49.
24. George, D.; Mallery, P. *IBM SPSS Statistics 23 Step by Step: A Simple Guide and Reference*, 14th ed.; Routledge, Taylor & Francis Group: London, UK, 2016; pp. 169–176.
25. Fang, H.; Niu, M.; Wang, X.; Zhang, Q. Effects of reduced chemical application by mechanical-chemical synergistic weeding on maize growth and yield in East China. *Front. Plant Sci.* **2022**, *13*, 1024249. [CrossRef]

26. Fang, H.; Zhang, Q.; Chandio, F.A.; Guo, J.; Sattar, A.; Arslan, C.; Ji, C. Effect of straw length and rotavator kinematic parameter on soil and straw movement by a rotary blade. *Eng. Agric. Environ. Food* **2016**, *9*, 235–241. [CrossRef]
27. Fang, H.; Ji, C.; Ahmed, A.T.; Zhang, Q.; Guo, J. Simulation analysis of straw movement in straw-soil-rotary blade system. *Trans. Chin. Soc. Agric. Mach.* **2016**, *47*, 60–67.